Geant4 Modeling of Cellular Dosimetry of [188]Re: Comparison between Geant4 Predicted Surviving Fraction and Experimentally Surviving Fraction Determined by MTT Assay

Sara Mohammadi[1] , Mahdy Ebrahimi Loushab[2], Mohammad Taghi Bahreyni Toossi[3]*

[1]PhD, Department of Medical Physics, Mashhad University of Medical Sciences, Mashhad, Iran
[2]PhD, Department of Physics, Faculty of Rajaee, Quchan Branch, Technical and Vocational University (TVU), Khorasan Razavi, Iran
[3]PhD, Medical Physics Research Center, Mashhad University of Medical Sciences, Mashhad, Iran

ABSTRACT

Background: The importance of cellular dosimetry in both diagnostic and radiation therapy is becoming increasingly recognized.

Objective: This study aims to compare surviving fractions, which were predicted using Geant4 and contained three types of cancer cell lines exposed to [188]Re with the experimentally surviving fraction determined by MTT assay.

Material and Methods: In this comparative study, Geant4 was used to simulate the transport of electrons emitted by [188]Re from the cell surface, cytoplasm, nucleus or medium around the cells. The nucleus dose per decay (S-value) was computed for models of single cell and random monolayer cell. Geant4-computed survival fraction (SF) of cancer cells exposed to [188]Re was compared with the experimental SF values of MTT assay.

Results: For single cell model, Geant4 S-values of nucleus-to-nucleus were consistent with values reported by Goddu et al. (ratio of S-values by analytical techniques vs. Geant4 = 0.811–0.975). Geant4 S-values of cytoplasm and cell surface to nucleus were relatively comparable to the reported values (ratio =0.914–1.21). For monolayer model, the values of $S_{Cy \to N}$ and $S_{CS \to N}$, were greater compared to those for model of single cell (2%–25% and 4%–38% were larger than single cell, respectively). The Geant4 predicted SF for monolayer MCF7, HeLa and A549 cells was in agreement with the experimental data in $10 \mu Ci$ activity (relative error of 2.29%, 2.69% and 2.99%, respectively).

Conclusion: Geant4 simulation with monolayer cell model showed the highest accuracy in predicting the SF of cancer cells exposed to homogeneous distribution of [188]Re in the medium.

*Corresponding author:
Mohammad Taghi Bahreyni Toossi
Medical Physics Research Center, Mashhad University of Medical Sciences, Mashhad, Iran
E-mail: mbahreyni@gmail.com

Introduction

Ionizing radiation plays a crucial role in treating malignant diseases. However, the effectiveness of external beam radiotherapy in treatment of solid tumors has been shown, it has not been useful in man-

aging dispersed small tumors and micro metastasis.

Radionuclide therapy is a promising therapeutic procedure for treating some diseases. In radionuclide therapy, unsealed radionuclides delivered to patients cause the target cells to absorb radiation in a selective manner [1]. The cellular behavior of administered radionuclides is conventionally analyzed using radiobiological experiments. The values of absorbed dose are necessary to evaluate observed radiobiological impacts and make prediction or comparison of the efficiency of various radionuclides. Moreover, accurate computation of dose is vital for treatment planning in radiation therapy [2]. The primary concern in the success of radionuclide therapy is appropriate selection of pharmaceuticals for effective targeting of cancer cells and restricting the radiation dose to targeted tumors. Nevertheless, limiting the radiation dose to cancer cells is a complex process especially at small-sized tumor. Under this condition, the range of particles emitted from the radionuclide must be adequately small to prevent any damage to the neighboring normal tissues while the absorbed dose of tumors needs to be as uniform as possible for effective treatment. Achieving such a balance between particle range and tumor size entails a thorough knowledge of spatial distribution of radiation dose in the vicinity of the radionuclide at microscopic levels [3]. At this level, experimental dosimetry is almost infeasible and mathematical techniques are the only available option [4, 5]. There are two primary techniques of internal dose estimation, including analytical calculation and Monte Carlo simulation [6, 7].

Today, Monte Carlo simulation offers the most accurate technique of tracking the particles transport in inhomogeneous materials and is thus well suited for estimating energy transfer from particles to materials at microscopic level. Various Monte Carlo codes with different levels of complexity have been presented that many of them already utilized for cellular

dosimetry [8-12]. Nevertheless, current Monte Carlo codes are chiefly developed according to the condensed history algorithms with few codes working based on a track structure technique. In the former technique, a particle's tracks are divided into small segments and their interactions along tracks are averaged at the end of each segment. In the track structure technique, however, all interactions are considered in an event-by-event manner [13].

In theory, track structure codes yield more accurate results in comparison to the condense history code, but few studies have explored this type of Monte Carlo codes.

Geant4 represents the use of a track structure Monte Carlo code for simulating path of article through matters [14, 15], which is capable of tracking physical processes to extremely low energies in bio-molecules measurement, developing models for the description of biologic systems such as cells and DNA, as well as models for explanation of biologic procedures. Geant4 simulations offer a practical method to achieve accurate dose values by taking into account all irradiation aspects such as geometry and activity distribution. Such abilities make Geant4 superior to all other types of existing codes [16].

In this study, we used Geant4 toolkit for the simulation of the transport of the emitted electrons from the ^{188}Re isotopes in aqueous media and the geometry of the flask containing cells. Using calculating the absorbed dose in the nucleus of the cell (as the sensitive volume), in various radioactive distribution and the linear quadratic equation, we computed the survival fraction and compared the results of the simulated SF with that of the experimental SF.

Material and Methods

The Geant4 toolkit

In Geant4, since particles are tracked down to zero energy, simulation needs to be limited by production cut. Based on these thresholds, the transfer of minimal energy to a second-

ary particle is determined so that the secondary particle is incorporated in the simulation. Geant4 Version 10.3 patch 1 was used for all simulations.

In this comparative study, considering the cell and nucleus dimensions and the electron range generated by the [188]Re decay, we used the Livermore model with a production cut of 250 eV and a *Max-Step* of 5 μm, which is in most cases a track structure model [17]. "The *production cut* determines how many secondary electrons and gamma are transported by the application; on the other hand, the *Max-Step* parameter forces the step performed by any particle during its propagation: also in this case a small step means a big precision in the transportation but a long computation time"[18].

Evaluation of Geant4

To evaluate the precision and potentials of Geant4 for medical and radiobiological applications, S- values were computed for spheres in different sizes (as a various cell lines) [19]. The doses to the nucleus per decay of [188]Re from the nucleus ($S_{N \to N}$), cell surface ($S_{Cs \to N}$) and cytoplasm ($S_{Cy \to N}$) were determined for the models of single cell and random monolayer cell. The spheres, which consisted of water and a comparison with the results of MIRD, cell S-value for single cell model was shown in Table 1.

S-value computation

In order to simulate the cell and the nucleus, we assumed that they are two concentric spheres with different radii for three cell lines, as follows: A549, MCF7 and HeLa. Cell radii were considered 5.3, 9 and 10 μm and nucleus radii were 3.5, 6.5 and 5 μm [20-22]. For the simulation of the exposure to cells seeded into 96-well tissue culture plate, which contained 200 μl of culture medium, the interested volume for this study was considered as a cylinder with a diameter of 3.2 mm and a height of 7.32 mm that there is polystyrene lower 1 mm

of cylinder and the rest is water. A monolayer of cancer cells (consist of 5000 cells) was attached to the top of polystyrene. Only for imitating the cells in experiment, a random distribution of cells was used in monolayer model (Figure 1).

For each simulation, 10^9 decays were started to achieve a standard deviation of less than 1%. The total energy of particles, which was less than 250 eV, was deposited locally.

Primary particle generation

Radioisotope decays as a source of primary particles, and the activation of the radioactive decay physics with different distributions within the flask occurred and the particle transport was simulated with high precision. Rhenium-188 ([188]Re), as a β-emitting radionuclide, is commonly used in radio immunotherapy because of its enhanced radiation energy (maximum of 2.12 MeV for β⁻ and γ emission of 155 keV), suitable half-life (17.005 hours), and ease of production [23].

Calculation of cell survival fraction (SF

Cell survival curves (SF vs. absorbed dose), were to follow the linear quadratic model with the following equation:

$$SF = e^{-(\alpha D + \beta D^2)} \qquad (1)$$

In this equation, α and β represent constants and D is the absorbed dose. For each cell line, α and β constants were derived from the colony assay and D in equation 1 was presumed to represent the absorbed dose in the nucleus.

Cell lines and culture

A549, HeLa and MCF7 cell lines were purchased from the Pasture Institute of Iran. The cells were preserved as a monolayer in RPMI 1640 (Sigma) medium, including 10% fetal bovine serum (Sigma), 100 U/mL penicillin, 100 U/mL streptomycin, and 2 mM glutamine. The cell incubated at 37°C in a humidified atmosphere of 5% CO_2 in air were in the loga-

Table 1: S-Values (mGy/Bq-s) calculated by Geant4 and Medical Internal Radiation Dose (MIRD)

R_C (um)	R_N (um)	Single cell Geant4			Medical Internal Radiation Dose (MIRD)			Monolayer cell Geant4		
		$S_{(N \to N)}$	$S_{(Cy \to N)}$	$S_{(CS \to N)}$	$S_{(N \to N)}$	$S_{(Cy \to N)}$	$S_{(CS \to N)}$	$S_{(N \to N)}$	$S_{(Cy \to N)}$	$S_{(CS \to N)}$
3	2	5.612	0.956	0.478	5.00	1.07	0.578	5.597	0.978	0.502
3	1	32.07	1.300	0.400	26.0	1.47	0.459	31.87	1.318	0.421
4	3	2.023	0.454	0.266	1.88	0.601	0.305	2.031	0.473	0.286
4	2	5.614	0.532	0.228	5.00	0.601	0.245	5.598	0.552	0.247
5	4	0.989	0.265	0.171	0.943	0.321	0.157	1.004	0.282	0.190
5	3	2.022	0.291	0.150	1.88	0.321	0.157	2.029	0.310	0.167
5	2	5.607	0.347	0.141	5.00	0.383	0.144	5.597	0.364	0.159
6	5	0.574	0.173	0.120	0.553	0.187	0.131	0.588	0.190	0.137
6	4	0.990	0.185	0.106	0.943	0.200	0.110	1.002	0.202	0.123
6	3	2.021	0.209	0.101	1.88	0.226	0.102	2.029	0.226	0.118
7	6	0.369	0.123	0.089	0.359	0.131	0.096	0.385	0.139	0.106
7	5	0.573	0.128	0.080	0.553	0.137	0.082	0.588	0.144	0.096
7	4	0.990	0.141	0.076	0.943	0.150	0.076	1.003	0.157	0.092
7	3	2.022	0.159	0.073	1.88	0.170	0.073	2.029	0.175	0.089
8	7	0.256	0.092	0.069	0.250	0.097	0.073	0.271	0.107	0.085
8	6	0.370	0.095	0.062	0.359	0.100	0.063	0.380	0.110	0.078
8	5	0.573	0.102	0.059	0.553	0.107	0.059	0.588	0.117	0.074
8	4	0.990	0.112	0.057	0.943	0.118	0.057	1.002	0.128	0.073
9	8	0.187	0.071	0.055	0.183	0.074	0.058	0.202	0.086	0.070
9	7	0.256	0.073	0.050	0.250	0.076	0.051	0.271	0.088	0.065
9	6	0.370	0.078	0.048	0.359	0.081	0.047	0.384	0.093	0.062
9	5	0.573	0.084	0.046	0.553	0.087	0.046	0.587	0.099	0.061
10	9	0.142	0.057	0.045	0.140	0.059	0.047	0.157	0.071	0.060
10	8	0.187	0.058	0.041	0.183	0.060	0.041	0.201	0.072	0.555
10	7	0.256	0.061	0.039	0.250	0.063	0.039	0.271	0.075	0.054
10	6	0.370	0.065	0.038	0.359	0.067	0.037	0.383	0.080	0.052
10	5	0.573	0.071	0.037	0.553	0.073	0.036	0.587	0.085	0.051

rithmic growth phase at the initiation of the experiments.

MTT assay

The resuspension of cells was implemented at 2500 cells/200 μl in RPMI 1640 medium, and cultured in 96-well plate. After 24 h, the wells were supplemented with 0–150 μCi of [188]Re-perrhenate solution (the area between each two wells treated with Rhenium, was interleaved by empty wells filled with cell culture medium acting as the absorbing medium) and incubated for 1 h at 37°C. In the next step, wells were aspirated, and 200 μl of the medium was added to each well. 72 h after reaction, cell viability was estimated using MTT assay and an ELISA reader (microreader, Hyperion) at 540 nm and regarded as the percentage of
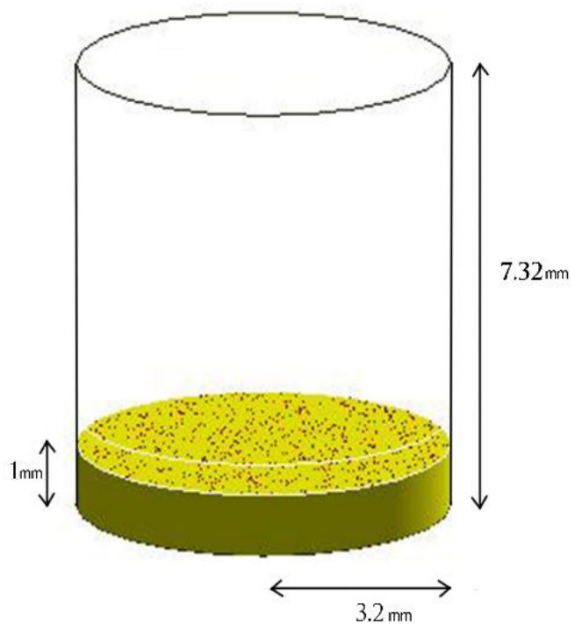
Figure 1: A single well of 96-well plate with a monolayer of cancer cells (red). Polystyrene is shown in yellow and cells are distributed over polystyrene randomly

viability. There were eight wells for each concentration of [188]Re and the experiment was replicated three times.

Colony formation assay

The experiments were conducted with cells from exponentially growing cultures by initial seeding of 3×10^5 cells into 10 ml of media in T-75 flasks. Based on the exponential phase declining, the cells were trypsinized and plated in 2 ml of media in a 6-well plate. The number of cells plated varied from 500 to 5000 depending on the different concentrations of [188]Re [24] and incubated overnight. In the following day, various concentrations of [188]Re-perrhenate solution was added to the growth medium and consequently eliminated by washing the cells and adding drug-free medium within 1 hr. Colony-forming units were identified 10 days later through staining with methylene blue (0.2%). Light microscopy was used to determine the number of colonies in each well. From the division of the number of colonies formed in the control wells to the number of seeded cells, the plating efficiency can be determined. In addition, to compute the SF value, one can multiply the plating efficiency to the division of the number of colonies by the number of cells seeded. The P values were estimated by the 2-tailed nonparametric t-test on the SFs in control and treated cultures. The mean-standard deviation of three experiments can be demonstrated by the data points and error bars shown in figures. To generate survival curves, a data analyzer software, Gunplot (version 4), was used and linear quadratic functions were fitted; in addition, alpha and beta constants were computed for each cell line.

Results

S-Values for [188]Re uniformly distributed in cell compartments

Single Cell Model

To investigate the possibility of applying the Geant4 to calculate subcellular S-values, we have calculated the dose to nucleus from [188]Re, which was uniformly distributed in cytoplasm, nucleus or on the cell surface compartments of a single cell in different dimensions. In Table 1, the comparison between the values calculated in this study with the values reported by Goddu et al. [25] has been shown. $S_{N \to N}$ reported by Goddu et al. was moderately smaller than those for Geant4 [25]. The majority of Geant4-computed $S_{Cy \to N}$ and $S_{CS \to N}$ were in the range published by Goddu et al. (ratio = 0.914–1.21) [25]. For a single cell of the similar radius, both $S_{N \to N}$ and $S_{Cy \to N}$ decreased if the radius of the nucleus increased. Besides, the decline of $S_{N \to N}$ was more pronounced than $S_{Cy \to N}$. The effect of the nucleus size on $S_{CS \to N}$ was more delicate than $S_{Cy \to N}$. For a single cell of identical nucleus radius, the cell radius did not have any impact on $S_{N \to N}$. Nevertheless, with an increase in the cell radius, both $S_{Cy \to N}$ and $S_{CS \to N}$ decreased. These trends were consistent with the ones reported by Goddu et

al. [25], as shown in Table 1.

Monolayer Cell Model

Experiments assessing the antiproliferative or cytotoxic effects of Auger electron emitting radiopharmaceuticals, usually involve the exposure of cells in a monolayer in culture plates instead of cell clusters or single cells. Thus, S-values to the nucleus of the cell were computed for ^{188}Re uniformly distributed in different cell compartments of random monolayer cell using Geant4 (Table 1) and then compared with the S-values for single cells. In S-values for monolayer cell, $S_{N \to N}$ were moderately smaller in comparison with those for single cell model. $S_{Cy \to N}$ and $S_{CS \to N}$, were greater than the calculated values for single cells (2%–25% larger for $S_{Cy \to N}$ and 4%–38% larger for $S_{CS \to N}$). Given the range of low-energy electrons, which are copious in number, radiation from particles deposited on the cell surface or inside the cytoplasm can reach the nucleus of adjacent cells and cause an increase in doses.

Survival Curves

For the evaluation of α and β constants, a survival curve was plotted based on the experimental data of colony assay (Figure 2). For each cell line, by fitting a linear quadratic equation in experimental data, α and β parameters of survival curve were obtained. For MCF7 (human breast adenocarcinoma cell line), HeLa (cervical cancer cell line) and A549 (non-small cell lung adenocarcinoma cells), α and β were 0.23(Gy^{-1}) and 0.06 (Gy^{-2}), 0.145 (Gy^{-1}) and 0.02 (Gy^{-2}), 0.21(Gy^{-1}) and 0.023(Gy^{-2}), respectively.

S-values for individual cancer cell lines

The S-value for the three MCF7, HeLa, and A549 cell lines with an error of less than 1% is depicted in Table 2. For distributing radioactivity in the nucleus, cytoplasm and on the cell surface with primary particle number of 2×10^9, we obtained an acceptable error. However, in the case of radioactivity distribution
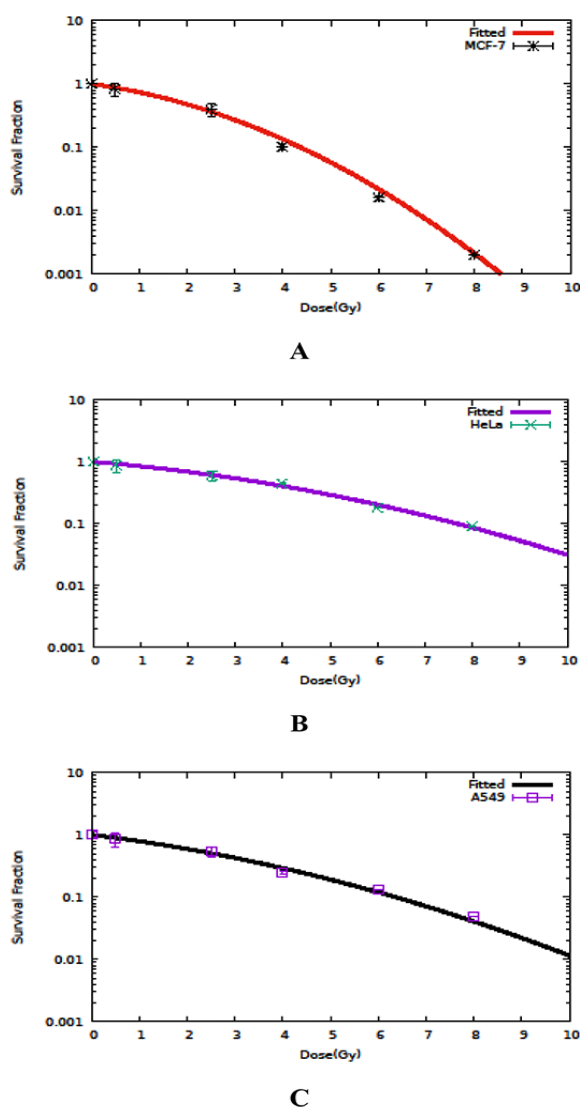
A

B

C

Figure 2: Radiation survival curves for each cell line. A) Michigan Cancer Foundation-7 (MCF7), B) HeLa., C) A549.

in the medium, the Monte Carlo error depends on the number of particles entered into the sensitive volume, and in this case, the number of particles reaching the nucleus is extremely low, to reach an error of less than 1%; in addition, it was run for 10^{10} primary particles.

Decreasing the size of cell nucleus leads into the increase in the value of $S_{(N \to N)}$ because the steady-state radioactivity is distributed at a smaller volume. The value of $S_{(Cy \to N)}$ decreases with a rise in cytoplasm volume. Furthermore, as A549 cell line contains the lowest cytoplas-

Table 2: S-Values (mGy/Bq-s) for individual cancer cell lines using monolayer cell model

Cell line	$S_{(N \to N)}$	$S_{(Cy \to N)}$	$S_{(CS \to N)}$	$S_{(Medium \to N)}$
MCF7	0.384	0.092	0.062	0.001024
HeLa	0.585	0.085	0.051	0.001022
A549	1.350	0.264	0.154	0.001011

MCF7: Michigan Cancer Foundation-7

mic volume, $S_{(Cy \to N)}$ is larger. The same rule applies to $S_{(CS \to N)}$.

Finally, a uniform radioactivity distribution was used to compare the results of the simulations with experimental studies. To do this, we defined $S_{(Medium \to N)}$ as the dose reaching the cell nucleus, which follows a Rhenium decay at a random point inside the flask. The decrease in the nucleus size causes $S_{(Medium \to N)}$ to be reduced. Although due to small size of the nucleus volume compared to the global dimensions and dispersion of radionuclide, the effect of the difference in nucleus dimensions (1.5 to 3 micrometers) on the value of $S_{(Medium \to N)}$ is very small, which is estimated at tenth of a percent (Table 2).

Comparison of Computed and Experimental SF

We compared the calculated SF of cancer cells, using Geant4 due to the exposure from [188]Re-perrhenate, with experimental ones. For this purpose, the cumulative radioactivity in cytoplasm, cell surface and in the nucleus was calculated based on the subcellular distribution of [188]Re in MCF7, HeLa and A549 cells. Then, the absorbed dose to cell nucleus was computed in terms of the obtained S-values, which were specific to these three cell lines. Finally, SF was derived and compared, as shown in Table 3.

To obtain the absorbed dose of nucleus derived from 10 µCi of Rhenium, $S_{(Medium \to N)}$ was multiplied by the equivalent number of decay (370000). Now, with of α and β constants and the linear quadratic equation, the survival fraction for each cell line was calculated. The same process was repeated for 75 and 150 µCi radioactivities and the results of simulation were compared with those obtained from the MTT assay (Table 3).

On the colony assay, a cell physically presenting in the biological system, with its capacity divided indefinitely and producing a large number of progenies, is lost and hence is considered "dead", while this type of cells is assigned to the live cells group in MTT assay. For this reason, the survival fraction obtained from MTT assay is greater than the one

Table 3: Comparison of calculated survival fraction (SF) with experimental SF for three cell lines

Cell line	Activity(µCi)	Geant4 calculated SF		experimental SF	
		Single cell	Monolayer cell	MTT assay	Colony assay
MCF7	10	0.92	0.91	0.88	0.81
	75	0.38	0.32	0.30	0.12
	150	0.07	0.04	0.11	0.00
HeLa	10	0.95	0.94	0.90	0.84
	75	0.59	0.56	0.49	0.18
	150	0.27	0.23	0.32	0.00
A549	10	0.93	0.92	0.91	0.89
	75	0.53	0.46	0.43	0.22
	150	0.22	0.15	0.28	0.02

SF: Survival fraction, MTT: Mean transit time, MCF7: Michigan Cancer Foundation-7

obtained from the colony assay. On the other hand, the absorbed dose calculated in Geant4 simulation is smaller than that of experiments because absorbed dose tends to be larger in the middle rather than the border of flask. Here, we calculated the absorbed dose in the border of flask (bottom) in Geant4 while the absorbed dose in the experiment was an averaged parameter. For example, in this study, 10 μCi of [188]Re was added to 200 μl of culture medium in a 96-well plate for 1 hour so that the averaged absorbed dose was equal to 0.8 Gy. Besides, the calculated absorbed dose of Geant4 was 0.37 Gy (Table 4). Finally, the Geant4 calculated SF was comparable to the MTT assay results.

In results of monolayer model, the estimated SF value was consistent with the experimental ones in 10 μCi. The single-cell model had low accuracy in predicting the SF. By contrast, the monolayer model turned out to be the very strong in predicting experimental SF, since this model has simulated the experimental conditions with more details.

Since the use of free radionuclides in the clinic is not common, if Rhenium is targeted with an existing strategy (monoclonal antibodies, nanoparticles, etc.) for cancer cells and the radioactivity is focused on the surface of cells, there will be a significant increase in the absorbed dose. In this study, for MCF7 cell line in 10 μCi radioactivity, the absorbed dose

for cumulative radioactivity on the cell surface would be 60 times greater than the radioactivity distribution in the medium, thereby leading to a significant reduction in the survival fraction of cancer cells. In the above case, the survival fraction drops from 90% to zero! (Table 4).

Discussion

Due changes of spherical shape in monolayer cells attached to the bottom of the flask, we simulated the cell and nucleus with two different geometries to determine the effect of this deformation. For this purpose, we simulated a spherical cell with a radius of 9 μm and a nucleus of 6.5 μm with a monolayer cell model and S-value was determined in the different distribution of radioactivities. Then the cell and nucleus with hemisphere and hemi ellipsoid shapes were considered. Although the volume of these new geometries was assumed to be same as previous spherical cells, the new size of the cell and nucleus was calculated and incorporated in the simulations. The change in the S-values obtained based on these deformed geometries was negligible (less than %2). In addition, our results show that the distribution of cells on the bottom of the flask did not make a significant difference in the S-values. We confirmed this point by applying two different methods of random distribution and placement at regular intervals, which result in less than %2 difference in S-values. In a fixed physical model (such as Livermore model), S-value depends on the number of cells and the dimensions of the cell and nucleus.

The number of cells in the flask in the monolayer model affects the S-value. Since only the cells number seeded is known, and the irradiation was launched 24 hours later, just an estimated number of cells were incorporated in the simulation.

The values of constants (α and β) were calculated by fitting the linear quadratic equation on the survival curve. AS the effect of these values on the obtained survival fraction was

Table 4: Geant4 calculated dose (Gy) and survival fraction (SF) in different radioactive distribution for 10 μCi of [188]Re

	In the medium		On the cell surface	
Cell line	Dose	SF	Dose	SF
MCF7	0.379	0.908704	22.94	*0.000000
HeLa	0.378	0.943936	18.87	0.000000
A549	0.374	0.921514	56.79	0.000000

SF: Survival fraction, MCF7: Michigan Cancer Foundation-7

*A micrometastasis (e.g. from 1 μg to 1 mg weight) may contain thousands to millions of cancer cells. So, the SF must be calculated down to at least 3 or even 6 significant digits.

extremely high, α and β values reported in several different papers [26-28] were studied on this cell lines. Given that the radiation used in this study consisted of electrons derived from the decay of the Rhenium isotope, α and β values differed from those reported in the aforementioned papers. This disparity can be attributed to the difference in the type of radiation in the study.

Geant4 displayed the highest flexibility in modeling different cell geometries in experimental contexts compared to analytical methods, capable of including various composition and density elements for the volumes under study. Analytical methods are only applicable to homogeneous medium and simple geometries.

This is the first paper to report Geant4 calculated SF of the cancer cells exposed to ^{188}Re and compare them with experimental data. The absorbed dose in the center of the flask is maximum and decreases by moving toward the sides; thus, the cells placed at the bottom of the flask receive lower dose than the average dose. In addition, this lower dose is important to predict the cell survival fraction and we determined the exact absorbed dose and SF for the three specific cell lines in this study.

Conclusion

Geant4 displayed the highest flexibility in modeling different cell geometries in experimental contexts and calculated absorption dose and SF of the cancer cells exposed to different isotopes.

Acknowledgment

Conflict of Interest

None

References

1. Chatal J-F, Hoefnagel CA. Radionuclide therapy. *Lancet*. 1999;**354**:931-5.

2. Schell S, Wilkens JJ, Oelfke U. Radiobiological effect based treatment plan optimization with the linear quadratic model. *Z Med Phys*. 2010;**20**:188-96. doi: 10.1016/j.zemedi.2010.02.003. PubMed PMID: 20832006.

3. Bousis C, Emfietzoglou D, Nikjoo H. Monte Carlo single-cell dosimetry of I-131, I-125 and I-123 for targeted radioimmunotherapy of B-cell lymphoma. *Int J Radiat Biol*. 2012;**88**:908-15. doi: 10.3109/09553002.2012.666004. PubMed PMID: 22348681.

4. Bardies M, Chatal JF. Absorbed doses for internal radiotherapy from 22 beta-emitting radionuclides: beta dosimetry of small spheres. *Phys Med Biol*. 1994;**39**:961-81. doi: 10.1088/0031-9155/39/6/004. PubMed PMID: 15551573.

5. Humm JL. Dosimetric aspects of radiolabeled antibodies for tumor therapy. *J Nucl Med*. 1986;**27**:1490-7. PubMed PMID: 3528417.

6. Humm JL. A microdosimetric model of astatine-211 labeled antibodies for radioimmunotherapy. *Int J Radiat Oncol Biol Phys*. 1987;**13**:1767-73. doi: 10.1016/0360-3016(87)90176-3. PubMed PMID: 3667382.

7. Emfietzoglou D, Bousis C, Hindorf C, Fotopoulos A, Pathak A, Kostarelos K. A Monte Carlo study of energy deposition at the sub-cellular level for application to targeted radionuclide therapy with low-energy electron emitters. *Nucl Instrum Methods Phys Res B*. 2007;**256**:547-53.

8. Bousis C, Emfietzoglou D, Hadjidoukas P, Nikjoo H. A Monte Carlo study of absorbed dose distributions in both the vapor and liquid phases of water by intermediate energy electrons based on different condensed-history transport schemes. *Phys Med Biol*. 2008;**53**:3739-61. doi: 10.1088/0031-9155/53/14/003. PubMed PMID: 18574312.

9. Bernal MA, Liendo JA. An investigation on the capabilities of the PENELOPE MC code in nanodosimetry. *Med Phys*. 2009;**36**:620-5. doi: 10.1118/1.3056457. PubMed PMID: 19292002.

10. Syme AM, Kirkby C, Riauka TA, Fallone BG, McQuarrie SA. Monte Carlo investigation of single cell beta dosimetry for intraperitoneal radionuclide therapy. *Phys Med Biol*. 2004;**49**:1959-72. doi: 10.1088/0031-9155/49/10/009. PubMed PMID: 15214535.

11. Cai Z, Pignol J-P, Chan C, Reilly RM. Cellular dosimetry of 111In using Monte Carlo N-particle computer code: comparison with analytic methods and correlation with in vitro cytotoxicity. *J Nucl Med*. 2010;**51**:462-70. doi: 10.2967/jnumed.109.063156.

12. Cai Z, Kwon YL, Reilly RM. Monte Carlo N-Particle (MCNP) Modeling of the Cellular Dosimetry of 64Cu: Comparison with MIRDcell S Values and Implications for Studies of Its Cytotoxic Effects. *J Nucl Med.* 2017;**58**:339-45. doi: 10.2967/jnumed.116.175695. PubMed PMID: 27660146.

13. Nikjoo H, Uehara S, Emfietzoglou D, Cucinotta F. Track-structure codes in radiation research. *Radiat Meas.* 2006;**41**:1052-74. doi: 10.1016/j.radmeas.2006.02.001.

14. Agostinelli S, Allison J, Amako Ka, Apostolakis J, Araujo H, Arce P, et al. GEANT4—a simulation toolkit. *Nucl Instrum Methods Phys Res A.* 2003;**506**:250-303.

15. Allison J, Amako K, Apostolakis J, Araujo H, Dubois PA, Asai M, et al. Geant4 developments and applications. *IEEE Trans Nucl Sci.* 2006;**53**:270-8.

16. Chauvie S, Francis Z, Guatelli S, Incerti S, Mascialino B, Montarou G, et al., editors. Models of biological effects of radiation in the Geant4 Toolkit. IEEE Nuclear Science Symposium Conference Record; San Diego, Calif: IEEE Service Center; 2006.

17. Kyriakou I, Emfietzoglou D, Ivanchenko V, Bordage M, Guatelli S, Lazarakis P, et al. Microdosimetry of electrons in liquid water using the low-energy models of Geant4. *J Appl Phys.* 2017;**122**:024303. doi: 10.1063/1.4992076.

18. Cirrone GP, Cuttone G, Mazzaglia SE, Romano F, Sardina D, Agodi C, et al. Hadrontherapy: a Geant4-based tool for proton/ion-therapy studies. *Prog Nucl Sci Technol.* 2011;**2**:207-12. doi: 10.15669/pnst.2.207.

19. Sefl M, Incerti S, Papamichael G, Emfietzoglou D. Calculation of cellular S-values using Geant4-DNA: The effect of cell geometry. *Appl Radiat Isot.* 2015;**104**:113-23. doi: 10.1016/j.apradiso.2015.06.027. PubMed PMID: 26159660.

20. Jiang RD, Shen H, Piao YJ. The morphometrical analysis on the ultrastructure of A549 cells. *Rom J Morphol Embryol.* 2010;**51**:663-7. PubMed PMID: 21103623.

21. Arya SK, Lee KC, Bin Dah'alan D, Daniel, Rahman AR. Breast tumor cell detection at single cell resolution using an electrochemical impedance technique. *Lab Chip.* 2012;**12**:2362-8. doi: 10.1039/c2lc21174b. PubMed PMID: 22513827.

22. Zhao L, Sukstanskii AL, Kroenke CD, Song J, Piwnica-Worms D, Ackerman JJ, et al. Intracellular water specific MR of microbead-adherent cells: HeLa cell intracellular water diffusion. *Magn Reson Med.* 2008;**59**:79-84. doi: 10.1002/mrm.21440. PubMed PMID: 18050315. PubMed PMCID: PMCPMC2730972.

23. Chen KT, Lee TW, Lo JM. In vivo examination of (188)Re(I)-tricarbonyl-labeled trastuzumab to target HER2-overexpressing breast cancer. *Nucl Med Biol.* 2009;**36**:355-61. doi: 10.1016/j.nucmedbio.2009.01.006. PubMed PMID: 19423002.

24. Carlone M, Wilkins D, Raaphorst P. The modified linear-quadratic model of Guerrero and Li can be derived from a mechanistic basis and exhibits linear-quadratic-linear behaviour. *Phys Med Biol.* 2005;**50**:L9-13. doi: 10.1088/0031-9155/50/10/l01. PubMed PMID: 15876677.

25. Goddu SM. MIRD Cellular S values: Self-absorbed dose per unit cumulated activity for selected radionuclides and monoenergetic electron and alpha particle emitters incorporated into different cell compartments. Reston: Society of Nuclear Medicine; 1997.

26. Qing Y, Yang X-Q, Zhong Z-Y, Lei X, Xie J-Y, Li M-X, et al. Microarray analysis of DNA damage repair gene expression profiles in cervical cancer cells radioresistant to 252 Cf neutron and X-rays. *BMC Cancer.* 2010;**10**:71. doi: 10.1186/1471-2407-10-71.

27. Lacoste-Collin L, Castiella M, Franceries X, Cassol E, Vieillevigne L, Pereda V, et al. Nonlinearity in MCF7 Cell Survival Following Exposure to Modulated 6 MV Radiation Fields: Focus on the Dose Gradient Zone. *Dose Response.* 2015;**13**:1559325815610759. doi: 10.1177/1559325815610759. PubMed PMID: 26740805. PubMed PMCID: PMCPMC4679192.

28. Jiang L, Xiong XP, Hu CS, Ou ZL, Zhu GP, Ying HM. In vitro and in vivo studies on radiobiological effects of prolonged fraction delivery time in A549 cells. *J Radiat Res.* 2013;**54**:230-4. doi: 10.1093/jrr/rrs093. PubMed PMID: 23090953. PubMed PMCID: PMCPMC3589931.